

*Full Length Research Paper*

# **Analysis of shaly sand reservoir rocks in the eastern Niger Delta Basin using geophysical well logs**

**Fozao K. F.<sup>1,2\*</sup>, Djieto-Lordon A. E.<sup>1</sup>, Ali E. A. A.<sup>1</sup>, Agying C. M.<sup>1</sup>, Ndeh D. M.<sup>3</sup>  
and Zebaze Djuka M. K.<sup>1</sup>**

<sup>1</sup>Petroleum Research Group, University of Buea, P. O. Box 063, Buea, Cameroon.

<sup>2</sup>Department of Petroleum Engineering, School of Engineering (NAHPI), University of Bamenda, Bamenda, Cameroon.

<sup>3</sup>Arab Center for Engineering Studies (ACES)-Abu Dhabi, Industrial City of Abu Dhabi (ICAD) 1, Abu Dhabi, UAE.

Received 7 October, 2018; Accepted 29 November, 2018

**Shales in the reservoir causes complications for the petrophysicist because they generally are conductive and mask the high resistance characteristic of hydrocarbons. Data from a suite of well logs were used to estimate the effect of reservoir shaliness on petrophysical parameters of some reservoir rocks of the eastern Niger Delta Basin. The log section was digitized using Neuralog software. Delineation of the productive clean and dirty formations, as well as mapping of the fluid contents of the possible reservoir zones was carried out using Interactive Petrophysics software. Fifteen shaly sand bodies were identified. It was observed that, shale correction leads to a significant change in petrophysical parameters. The results obtained indicate that, the Simandoux and Indonesian models used for the study are both suitable for water saturation, and hydrocarbon saturation analysis in shaly sands of this part of the Basin. The porosity results for the Indonesian and Simandoux models gave, respectively 0.14-0.23 and 0.22-0.28, while the hydrocarbon saturation results are 0.650-0.908 and 0.650-0.911 with permeabilities values of 1487.442-8881.697 mD and 1568.532-7451.592 mD for uncorrected and corrected permeability, respectively. Thomas-Stieber model shows that shale distribution in sands of the eastern Niger Delta Basin is mainly structural with few of disperse and laminar ones.**

**Key words:** Reservoir rock, Shaly sands, petrophysical parameters, well logs, models.

## **INTRODUCTION**

The present local and global increase in demand for energy has placed both pressure and greater challenge to increase energy supply. Most of this energy is derived from hydrocarbon resources. In an oil prone area like the Niger Delta, even though hydrocarbons are within the subsurface, they cannot impulsively gush to the surface when penetrated by a production well (Aigbedion and

Iyayi, 2007). On the contrary, most reservoir hydrocarbons reside in the pore spaces or open fractures of sedimentary rocks like sandstones. To produce them, detailed geological, petrophysical knowledge and data are needed to guide the placement of the well paths (Stat Oil Research Group, 2003). This can consequently help to optimize hydrocarbon recovery, and to improve

\*Corresponding author. E-mail: [kfozao@gmail.com](mailto:kfozao@gmail.com). Tel: +237 675 397 789.

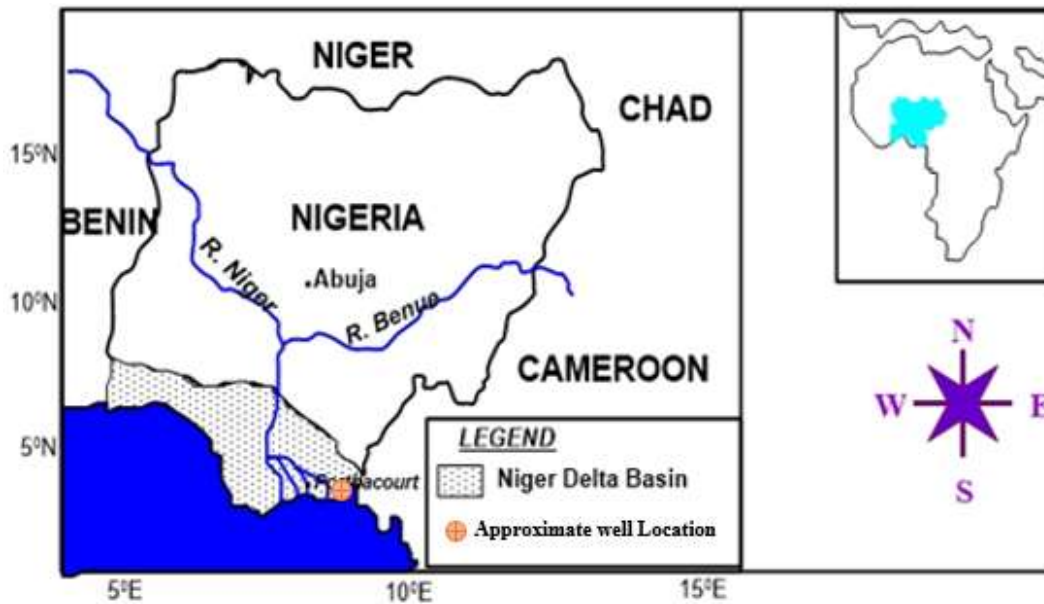


**Figure 1.** Map of Nigeria, showing the study area. Source: modified after Agyingi et al. (2013).

predictions of reservoir performance.

The Niger Delta region is known for its proficiency in hydrocarbon production among the sedimentary basins in Nigeria. Three major stratigraphic units have been recognized in the Niger Delta oil and natural gas province, namely Akata, Agbada and Benin Formations (Short and Stauble, 1967). Petroleum in the Niger Delta is produced from sandstones and unconsolidated sands predominantly in the Agbada Formation. Reservoir rocks are of Eocene to Pliocene in age, and are often stacked, ranging in thickness from less than 15 to 45 m thickness (Evamy et al., 1978). The primary source rock is the upper Akata Formation, the marine-shale facies of the delta, with possible contribution from interbedded marine shale of the lowermost Agbada Formation. The Niger Delta province contains only one identified petroleum system (Kulke, 1995) referred to as Tertiary Niger Delta (Akata-Agbada) Petroleum System.

The concept of shale differs from one discipline to another. To a reservoir engineer, shale can generally be characterized as low permeability formation. In most reservoirs, there exist a certain volume of shale, thus leading to unclean sandstone. Such reservoir rocks are termed shaly sands. Shale can be distributed across a reservoir sand body as a combination of different modes: laminar, structural or dispersed shale (Maeland, 2014). Shales can cause complications for the petrophysicist because they are generally conductive and may therefore mask the high resistance characteristic of hydrocarbons. Using Archie's equation in shaly sands results in very high water saturation values and may lead to potential hydrocarbon bearing zones being missed. The way shaliness affects log responses depends on the

proportion of shale, the physical properties of shale, and the way it is distributed in the host layer (Toby, 2005).

The prominent identity of the Niger Delta in Nigeria and in the world at large with respect to its hydrocarbon reserves, calls for proper exploration and petrophysical characterization, especially of the shaly sands which have been the subject of few research works in the past years. The main objective of this work is to use selected shaly sand analysis models to quantify the influence of shaliness on the petrophysical parameters of a productive formation. Petrophysical characterization using the considered shaly sand analysis models will enable a better evaluation of the reservoir quality and potential of the studied field in this part of the Basin. Reservoir zones that could have been lost will be identified. This will equally give a better understanding of the reservoirs of the area, and increase the certainty in the quantity of recoverable hydrocarbons in the basin.

### Geological setting

The Niger Delta is situated at the apex of the Gulf of Guinea on the west coast of Africa (Hamada, 1999; Doust, 1990) and on Nigeria's South-South geopolitical zone, in a rift triple junction related to the opening of the south Atlantic in the late Jurassic to the Cretaceous. According to Nwachukwu and Chukwura (1986), the Niger Delta is located in West Africa between latitude 3° and 6° N and longitude 5° and 8° E (Figure 1).

The Niger Delta is located geologically within 6 major geologic features: Gulf of Guinea, West African shield, Benin hinge line, Anambra basin, Abakaliki fold belt, and

the Calabar shield (Doust and Omatsola, 1990).

## METHODOLOGY

This work focuses on the interpretation of a composite geophysical well log section, obtained in a well in one of the offshore oil fields of the Niger Delta Basin (Figure 1), to delineate productive formations, as well as evaluating the influence of shaliness on formation petrophysical parameters. Three main tracks of this log section (lithology track, resistivity track, and the neutron and density porosity tracks) were analyzed.

The various lithologies through the log profile were deduced using the gamma ray log. This was achieved by setting a shale baseline and sand base line. Any deflection that touches the shale base line is that of a clean shale formation and any deflection on the sand line, is that of a clean sand formation. Intermediary deflections were considered as deflections of complex lithology formations.

According to Schlumberger (1989), gas or light hydrocarbons cause the apparent porosity from the density log to increase (resulting from a decrease in bulk density), and the porosity from the neutron log to decrease.

The log section was digitized using Neuralog software. The software that was used to delineate the productive clean and dirty formations, as well as mapping the fluid contents, was Interactive Petrophysics software. The behavior of the gamma ray log in different lithologies as modelled by Paul (2018), was from the deep and shallow resistivity logs (Dual Laterolog) of track 5, and confirmed by the porosity logs of track 9 in the log profile. A cross over between the density and neutron log readings indicates the presence of gas as confirmed by the high resistivity reading of gas in the resistivity log. The presence of a liquid is observed when two log readings come together or merge or do not cross over at all. The resistivity log (Schlumberger, 1972) is then used to confirm whether it is oil or water.

The flow chart showing the sequence of procedures is illustrated in the Appendix (Figure A). The following formulas were used for the calculation of petrophysical parameters:

The gamma ray index,  $I_{GR}$  was calculated using Equation 1 (Asquith and Gibson, 1982).

$$I_{GR} = \frac{(GR_{log} - GR_{min})}{(GR_{max} - GR_{min})} \quad (1)$$

In this equation,  $GR_{max}$ ,  $GR_{min}$  and  $GR_{log}$ , correspond to the maximum, minimum, and log read values of the gamma ray. The Larionov equation (Larionov, 1969) for shale volume ( $V_{sh}$ ) calculation in Tertiary rocks was then used to derive the shale volume (Equation 2).

$$V_{sh} = 0.083 * (2^{3.7 * I_{GR}} - 1) \quad (2)$$

To calculate the neutron, density and effective porosities, the following formulas were used. The density porosity ( $\phi_d$ ) was calculated using Equation 3.

$$\phi_d = \frac{\rho_{ma} - \rho_b}{\rho_{ma} - \rho_f} \quad (3)$$

where  $\rho_{ma} = 2.65$  g/cc,  $\rho_w = 1$  g/cc,  $\rho_{sh} = 2.66$  g/cc,  $\rho_g = 0.6$  g/cc,  $\rho_{oil} = 0.8$  g/cc, and  $\phi =$  apparent porosity;  $\rho_{ma} =$  matrix density;  $\rho_b =$  bulk density;  $\rho_f =$  fluid density.

The neutron porosity ( $\phi_n$ ) was read directly from the neutron log. To correct for shale effects on porosity, the corrected neutron ( $\phi_{nc}$ ) and density ( $\phi_{dc}$ ) porosities were derived using Equations 4 and 5.

$$\phi_{dc} = \phi_d - V_{sh} * \phi_{dsh} \quad (4)$$

$$\phi_{nc} = \phi_n - V_{sh} * \phi_{nsh} \quad (5)$$

where  $\phi_{dsh}$  and  $\phi_{nsh}$  are the corresponding porosity values in adjacent shales.

The following procedures were used to calculate the effective porosity  $\phi_e$ :

1) If  $\phi_{nc} > \phi_{dc}$ , there is no gas crossover, then, effective porosity is calculated using Equation 6.

$$\phi_e = (\phi_{nc} + \phi_{dc}) / 2 \quad (6)$$

2) If,  $\phi_{nc} < \phi_{dc}$ , there is gas crossover, then effective porosity is calculated using Equation 7:

$$\phi_e = \left[ \frac{\phi_{nc}^2 + \phi_{dc}^2}{2} \right]^{\frac{1}{2}} \quad (7)$$

where  $\phi_e$  is the numerical value of effective porosity after a cross plot of  $\phi_{dc}$  and  $\phi_{nc}$ .

The Archie equation (Equation 8), Simandoux (1963) model (Equation 9) and the Indonesian model (Poupon and Leveau, 1971) (Equation 10), were used to calculate water saturation ( $S_w$ ) and to estimate the shale effect on water saturation. The Simandoux and Indonesian models were used to correct for the presence of shale and its effects on water saturation as opposed to the Archie equation which is used for clean sands neglecting the presence of shale and its effects on the water saturation.

$$S_w = \sqrt{\frac{F * R_w}{R_t}} \quad (8)$$

where  $R_w =$  resistivity of the formation water;  $R_t =$  true formation resistivity;  $F =$  formation factor =  $a/\phi^m$ .  $a = 1$  for shale and 0.62 for sand,  $m = 2$  for shale and 2.15 for sand, and  $n = 2$ .

$$S_w = \frac{C * R_w}{\phi_e^2} \left[ \sqrt{\frac{5 \phi_e^2}{R_w R_t} + \left( \frac{V_{sh}}{R_{sh}} \right)^2} - \frac{V_{sh}}{R_{sh}} \right] \quad (9)$$

where  $C = 0.40$  for sand and 0.45 for carbonate;  $V_{sh} =$  lowest of the various shale indicators;  $R_t =$  deep resistivity (corrected for invasion);  $R_{sh} =$  deep resistivity reading in adjacent shale;  $\phi_e =$  effective porosity.

$$\frac{1}{\sqrt{R_t}} = \left[ \frac{V_{sh}^{1 - \frac{V_{sh}}{2}}}{\sqrt{R_{sh}}} + \frac{\phi_e}{\sqrt{R_w}} \right] * S_w \quad (10)$$

The permeability was calculated using Equation 11 (Tixier, 1949).

$$K = a \left[ \frac{\phi^b}{S_{wirr}^c} \right] \quad (11)$$

where  $S_{wirr}$  is the irreducible water saturation,  $a = 10000$ ,  $b = 5.0625$ , and  $c = 2$  from Schlumberger Chart K3;  $\Phi$  (non-corrected and corrected porosity) (Schlumberger, 1997, 2009).

The hydrocarbon saturation was calculated using Equation 12.

$$S_h = 1 - S_w \quad (12)$$

$$S_{wirr} = \frac{\phi}{D} \quad (13)$$

where  $D = 0.02$  to 0.1 from (Buckles, 1965).

In the absence of core data, the Thomas-Stieber model (Moradi et al., 2016; Thomas and Stieber, 1975; Dejtrakulwong et al., 2009) was used to establish the clay/shale distribution (dispersed, laminar and structural) within the zones of interest in the study area as illustrated in Figure 2.

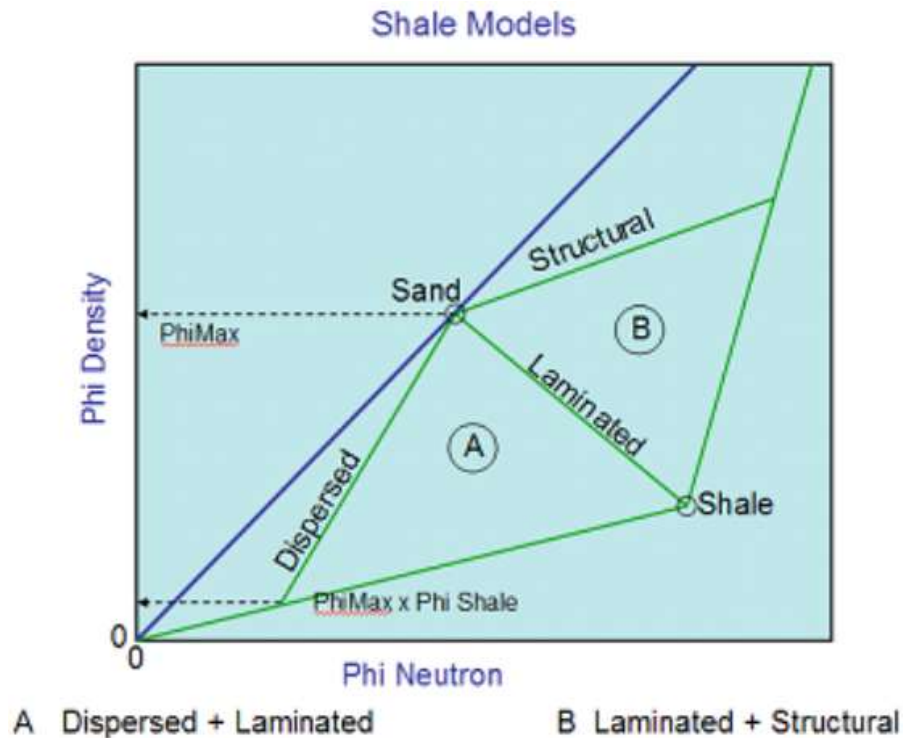


**Figure 2.** Thomas-Stieber model.

Source: Moradi et al. (2016), Thomas and Stieber (1975), and Dejtrakulwong et al. (2009).

## RESULTS AND INTERPRETATION

The results from Interactive Petrophysics were exported as input into the Microsoft Excel sheet, and various plots of the petrophysical parameters, against volume of shale were made. The goal of this approach is to clearly illustrate the changes in the values of the petrophysical parameters calculated, after shale corrections were made, and the variation of these parameters with changes in the shale volume.

### Fluid content and lithology deduction

After using the outlined methods, twenty eight potential reservoirs were identified, fifteen of which are shaly sands (grey bed colors) (Figure 3a-c) and with shale volumes ranging from 10.77 to 25.09% and thirteen clean sands (yellow bed colors) (Figure 3a-c), with shale volumes ranging from 3.42 to 10.05% (Figure 3a-c). The log section runs from a depth of 5764.44 to 8195.44 ft (1757 to 2498.97 m), with the maximum reservoir thickness of 75 ft (22.86 m) recorded for bed 64 with a depth of 6982.94 to 7057.94 ft (2128.4 to 2151.3 m), and minimum reservoir thickness of 12.25 ft (3.73 m) recorded for bed 80 with a depth of 8007.94 to 8028.94 ft (2440.8 to 2447.2 m), as indicated. These alternating sand and shale units correspond to the Agbada Formation

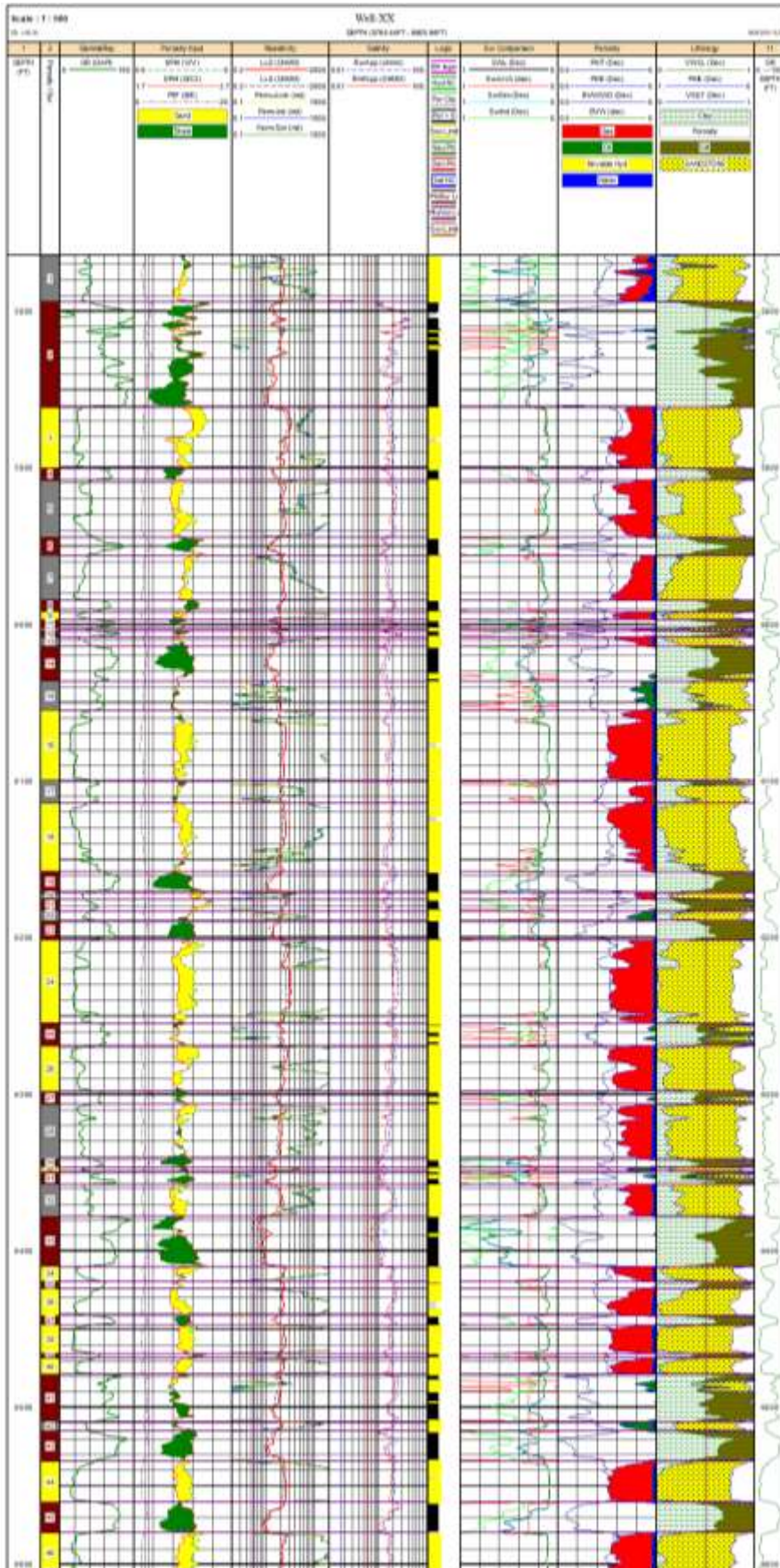
of Short and Stauble (1967).

The lithological log section shows an intercalation of thin sand and shale beds, as well as medium thick sands and shales, with thick to very thick shale formations below the depth of 7526.44 ft (2294.059 m) (Figure 3a-c). The reservoirs are mainly saturated with natural gas and water, as proven by the high resistivity readings,  $\phi_{nc}$  and  $\phi_{dc}$  values, the neutron-density cross separations and the  $S_h$  and  $S_w$  values. The reservoirs with gas contents, are characterized by high resistivity values (deep resistivity).

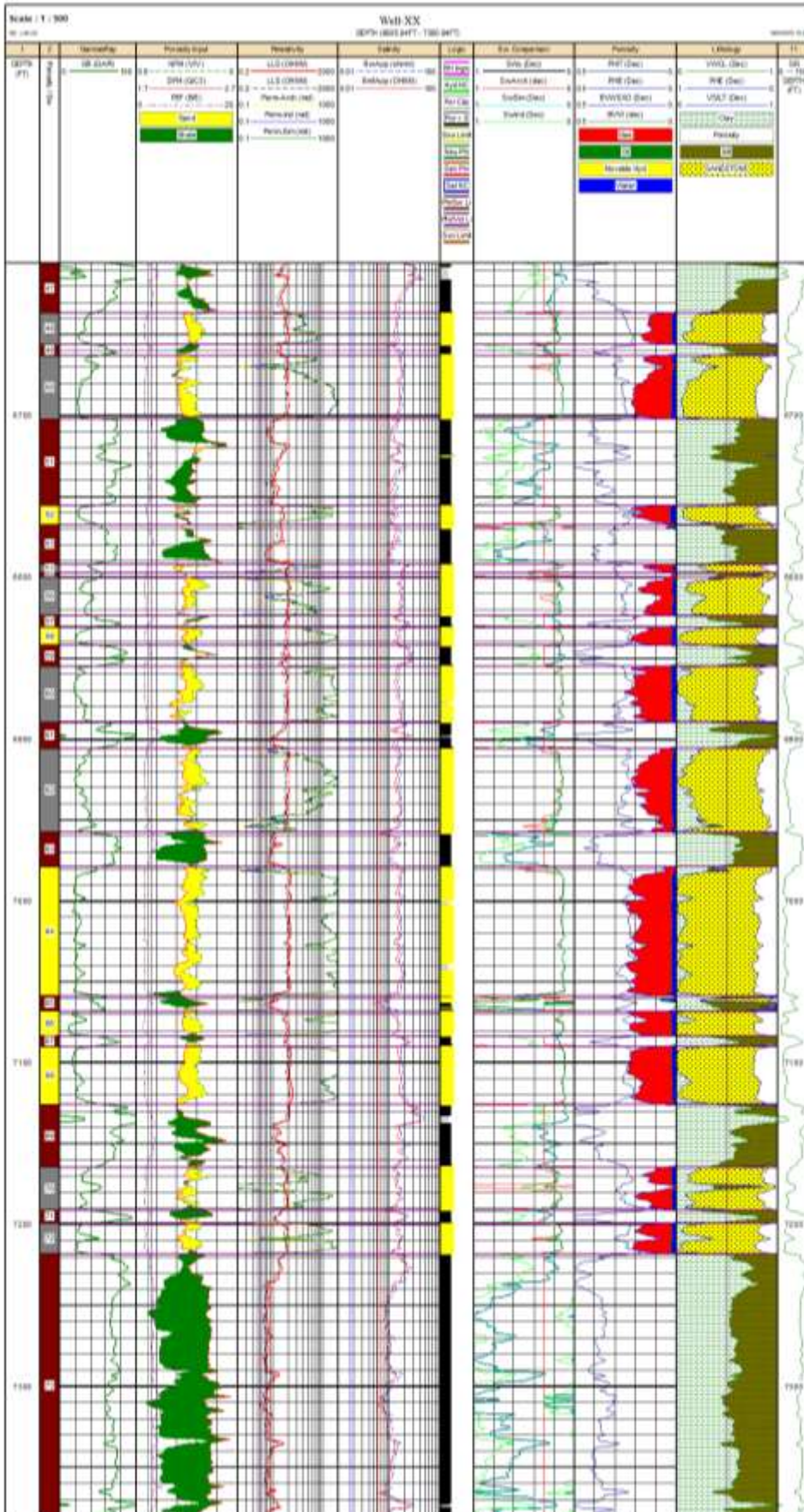
### Effects of reservoir shaliness on porosity

The influence of reservoir shaliness on effective porosity was determined using Equations 6 and 7 for effective porosity calculations. Obtained values were plotted against shale volume (Figure 4a and b). From Figure 4a, it can be seen that as the amount of shale ( $V_{sh}$ ) changes from a minimum value of 3.42 to 25.09% with a mean of 12.62%, the uncorrected effective porosity ( $\phi_e$ ) changes from 21.99 to 29.34% with a mean of 24.98%, and the corrected  $\phi_e$  changes from 22.25 to 28.32% with a mean value of 25.42% (Figure 4b).

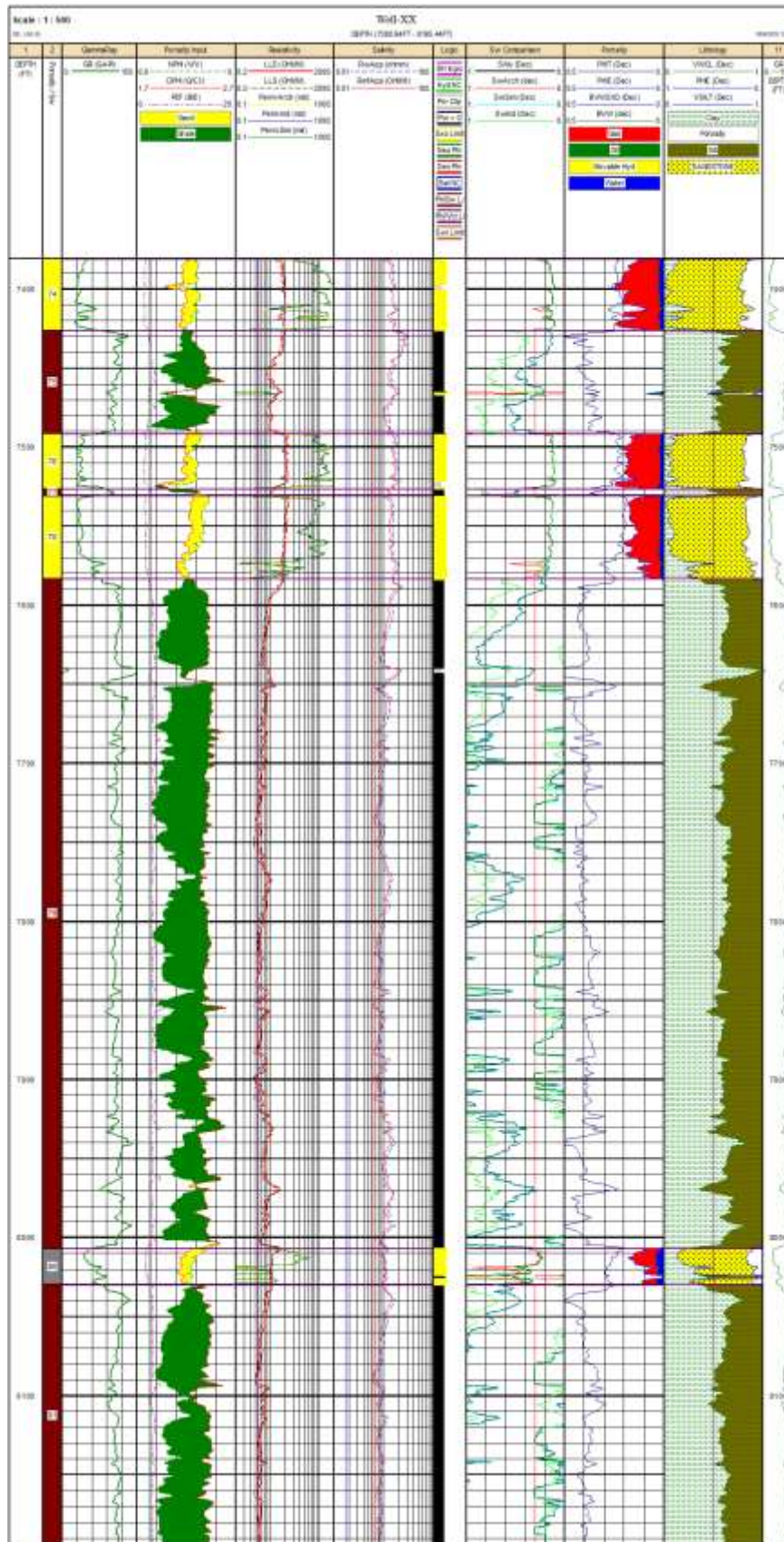
From the log interpretation and calculations made, the general trend of porosity (effective porosity), the uncorrected effective porosity shows an increase with



a



b



C

Figure 3. (a-c) Lithology and fluid modelling by well log interpretation, from 5764.44 to 8195.44 ft of depth through the log profile.

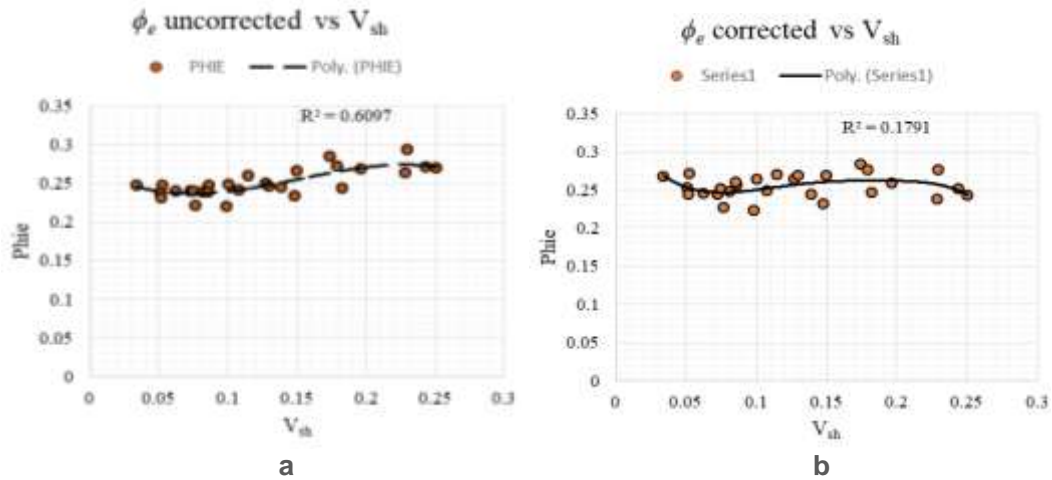


**Figure 4.** (a) Shale effect on uncorrected effective ( $\phi_e$ ) porosity, (b) Shale effect on corrected effective ( $\phi_e$ ) porosity.

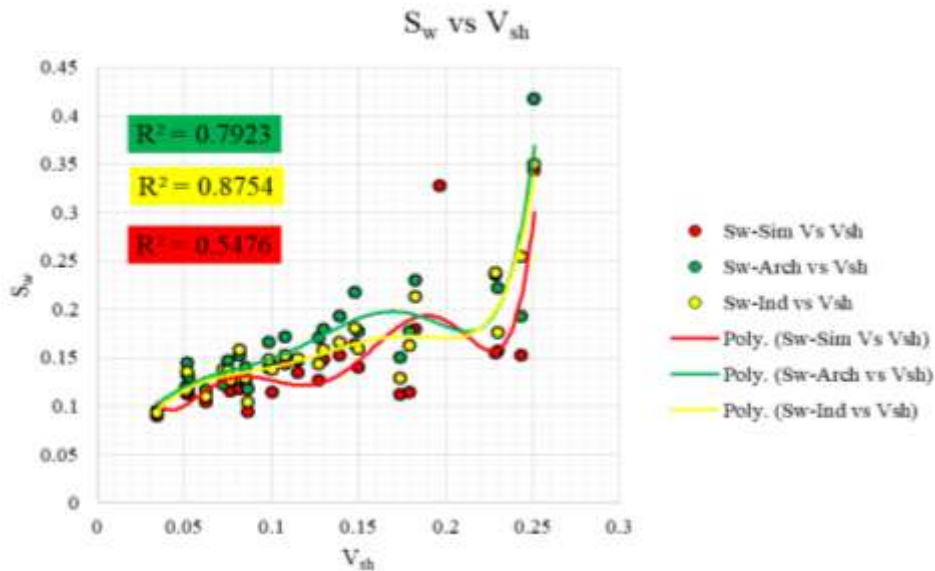


**Figure 5.** Influence of shale on water saturation.

increase in shale volumes (Figure 4a) with a positive regression coefficient ( $R^2$ ) of 0.61. The high values of  $\phi_e$ , signify that the presence of shale in sandstone reservoirs, overestimates the porosity, that is, it causes the logging tool to read higher porosities than are the porosities available for storage and circulation.

The corrected effective porosity shows a small increase with an increase in shale volumes (Figure 4b) with a positive regression coefficient ( $R^2$ ) of 0.179 which is negligible. This shows that the more the shale volume, the higher the uncertainty of actual porosity of the reservoir, which will affect the reservoir productivity potential.

### Effect of reservoir shaliness on fluid (water and hydrocarbon) saturation

The influence of reservoir shaliness on water saturation was determined using Equations 8, 9 and 10, for computing the Archie, Simandoux, and Indonesian water saturations, respectively (Sw-Arch, Sw-Sim and Sw-Ind), after which obtained values were plotted against shale volume (Figure 5). From Figure 5, it can be seen that as the amount of shale ( $V_{sh}$ ) changes, the Archie water saturation changes from 0.100 to 0.420 with a mean of 0.170, the Indonesian water saturation changes from 0.092 to 0.350 with a mean of 0.160, and the Simandoux



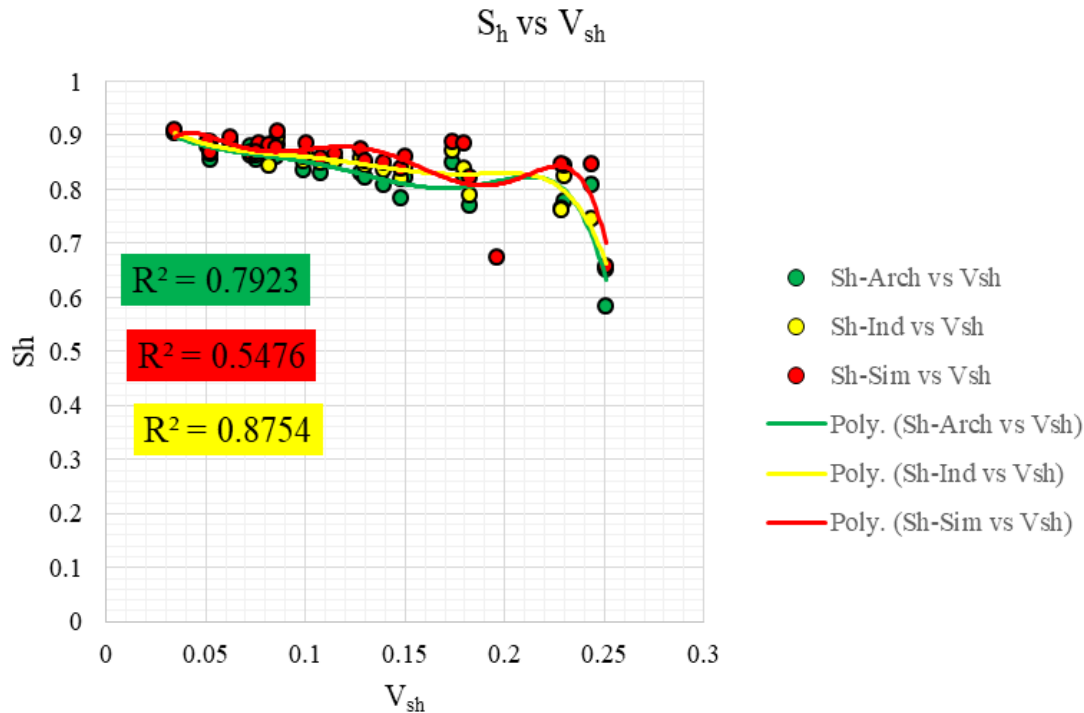


**Figure 6.** Influence of shale on hydrocarbon saturation.

water saturation changes from 0.089 to 0.340 with a mean value of 0.140.

The results show hydrocarbon saturations of the 0.580 to 0.900 with a mean of 0.830 for Archie; 0.650 to 0.908 with a mean of 0.840 for Indonesian, and 0.650 to 0.911 with a mean value of 0.840 for Simandoux (Figure 6). Results of hydrocarbon saturation ( $S_h$ ), show a decreasing but relatively constant trend with increasing shale volume for all the three models: Archie model ( $S_h$ -Arch), Indonesian ( $S_h$ -Ind) and Simandoux model ( $S_h$ -Sim) (Figure 6). However, the values of hydrocarbon saturation increase simultaneously from Archie, to Indonesian, and then to Simandoux model at a given values of shale volume (Figure 6).

#### Effect of reservoir shaliness on permeability

The influence of reservoir shaliness on permeability was determined using Equation 11 for computing the permeabilities. Values for  $\Phi$  were substituted in Equation 11 to obtain the estimated permeabilities corrected for shale and shale-non-corrected permeabilities, respectively (K-C and K-NC). Obtained values were plotted against shale volume (Figure 7). From Figure 7, it can be seen that as the amount of shale ( $V_{sh}$ ) changes, the shale non-corrected permeability changes from 1487.442 to 8881.697 mD with a mean of 3660.76 mD; the shale corrected permeability changes from 1568.532 to 7451.592 mD with a mean of 3900.466 mD.

#### Shale distribution

The distribution of shale is mainly structural with few dispersed and laminated shales (Figure 8)

#### DISCUSSION

The interpretation of shaly-sands log data has long been a challenge. As a result, there are more than 30 shaly-sand interpretation models, which have been developed in the last 50 years. Interpretation difficulties arise whenever the portions of clay minerals in a shaly-sand formation are high (Adeoti et al., 2015). This study employed 3 of those models, namely; complex lithology model for porosity correction, and the Indonesian, and Simandoux models for shale corrections of formation water saturation.

According to Bijan et al. (2010), an economical reservoir has cut off values of  $k = 1.0$  mD for lower cut off value,  $\phi = 10$ -12.5% for lower cut off value,  $S_w = 50$ -60% for upper cut off value, and  $V_{sh} = 27$ - 50% for upper cut off value. Results of this work after correction show, effective porosities ranging averagely from 22.25 to 28.32%, which according to Ulasi et al. (2012), are very good values. Permeability ranges from 1487.442 to 8881.697 mD,  $V_{sh}$  values ranges from 3.42 to 25.09%, and  $S_w$  values range from 8 to 34%, thus pointing to economic reservoir, if proper cost effective exploration and exploitation techniques are applied.

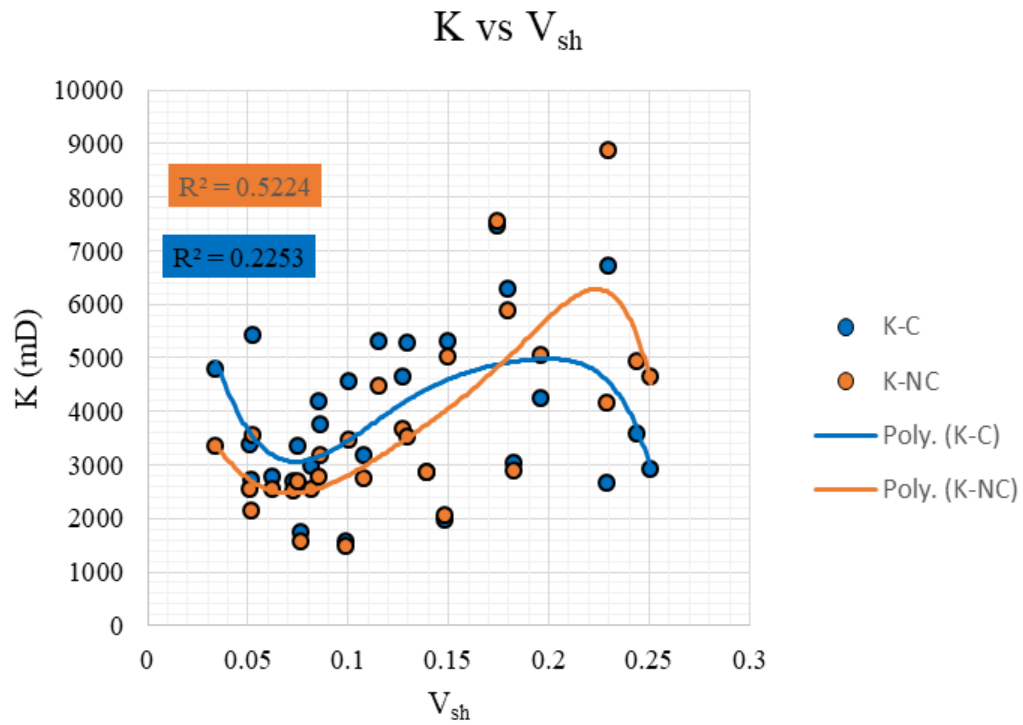


Figure 7. Influence of shale on permeability.

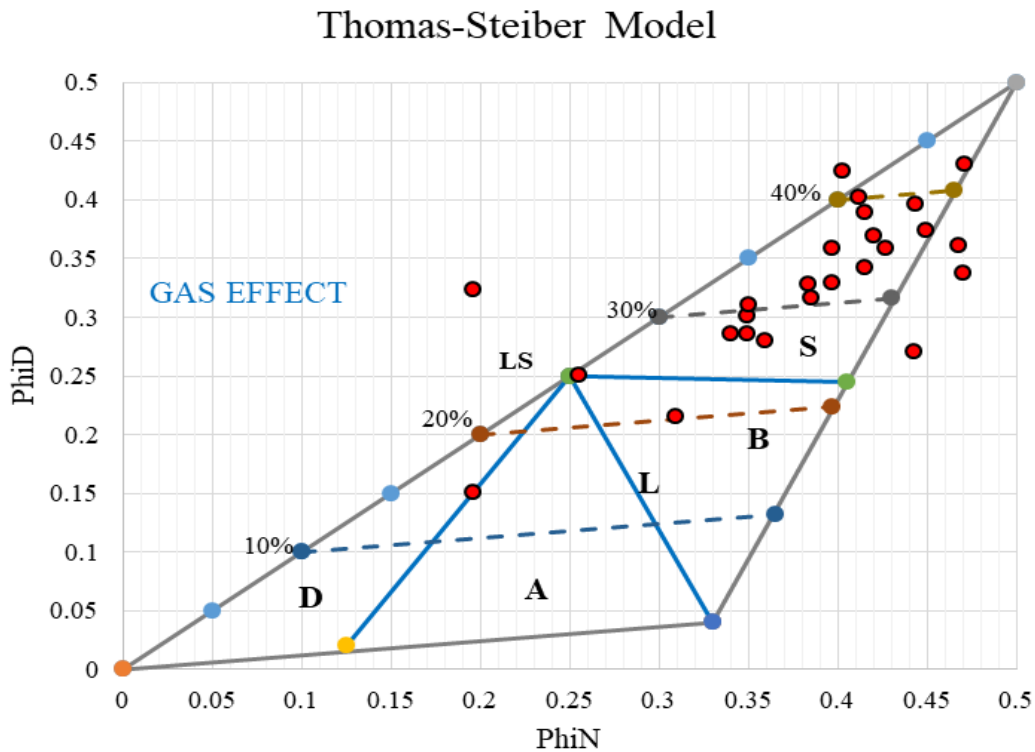


Figure 8. Thomas-Steiber model (modified from Moradi et al., 2016). Shale distribution from a neutron porosity-density porosity cross plot. Most of the points plot in the zone labeled "S" which corresponds to structural shale. However, with few dispersed and laminated shales. Some few points are subjected to 'gas effect'. Where A = dispersed + laminated, B = laminated + Structural, D = dispersed, L = laminated and S = structural.

## Porosity trends

Results of this work show an increase in effective porosity (uncorrected), with increase shale volume. This increase in porosity with increase in shale volume, can be accounted for by the fact that shales has its own porosity, and add to the sand porosity in the reservoir. This result does not agree with that of Adeoti et al. (2015), which shows a decrease in effective porosity against increase in shale volume, but agrees with the results obtained by Alao et al. (2013), which reiterated that effective porosity after shale correction is lower than the log derived porosity. According to Kurniawan (2002), clay minerals can cause the log-derived porosity values to be too high because of the limitation of density tool calibration whenever clay minerals are present; and because the high concentration of hydrogen ion in clays translate to a higher calculated porosity in neutron log tools. This thus could account for the reason why effective porosities (shale corrected porosities), are lower than the effective porosities derived from the logs.

The values for effective porosity obtained in this work, range averagely from 22.25 to 28.32%, and are very high. These results agree with conclusions made by Selley and Morrill (1983) and Egeh et al. (2001) which concluded that, almost all reservoirs have porosity in a range of 5 to 30%.

## Permeability

In a large number of studies on oil drilling, the existence of a positive correlation between permeability and porosity is identified (Nelson, 1994; Ehrenberg et al., 2006). The effect of shale on porosity is directly proportional to shale effect on permeability. Because of the intrinsic low permeability of shales, their presence in the reservoir reduce the connectivity between pores. Thus, an increase in shale volume reduces permeability in a reservoir.

## Fluid saturation

During water saturation interpretation, difficulties arise whenever the portions of clay minerals in a shaly-sand formation are high. These clay minerals contribute to an increase of the overall conductivity. In large quantities, their conductivity becomes as important as the conductivity of the formation water (Kurniawan, 2002). An increase in formation conductivity due to the presence of shale in a reservoir reduces the formation true resistivities ( $R_t$ ) and thus causes the derived water saturations ( $S_w$ ) to be seemingly higher, since water saturation and formation true resistivity have inverse relations.

According to Alao et al. (2013), Archie's equation was

developed for clean rocks, and it does not account for the extra conductivity caused by the clay present in shaly sands. Therefore, Archie's equation would not provide accurate water saturation in shaly sands.

Using Archie's equation in shaly sands results in very high water saturation, thus the Simandoux and Indonesian model were used in this work to correct for the high water saturation values. The log derived formation water saturation shows decreasing values from Archie's model to Indonesian model, and then to Simandoux model. From the results, the Simandoux model also shows higher values of hydrocarbon saturation. These results agree with that of Adeoti et al. (2015), which concluded that, the Simandoux and Indonesian models provide favorable petrophysical parameters indicating higher hydrocarbon potential than Archie model. This implies that the Simandoux and Indonesian model could be valuable tools in shaly sand environments.

## Shale distribution

Using the Thomas-Stieber model, the distribution of shale appears to be mainly structural with few dispersed and laminated shales. Some few points are subjected to 'gas effect'. The presence of structural shales increases the porosity of the reservoirs with increase in shale volume. In fact, structural shale are present as grains within the sand, which are similar to the findings of Thomas and Steiber (1975) and Mæland (2014) where the effective porosity in shaly sand are greater compared to those in clean sand.

## Conclusion

It can be concluded that shales in a reservoir formation is like scales in the human observation. In fact, shales can cause complications in interpretation for the petrophysicist because of their general conductivity and low permeability. As a result, the high resistance characteristics of hydrocarbons may be masked, leading to potential hydrocarbon zones being missed out.

After proper log analysis and interpretation, 28 potential reservoir zones (with 15 shaly and 13 clean) were identified. The stratigraphic unit from where the log data was derived is mainly composed of an intercalation of shales and sandstones corresponding to the Agbada Formation of Short and Stauble (1967). Utility and analysis of the shaly sand correction methods, point to the conclusion that the complex lithology model is suitable for shale corrections of the reservoir porosity and permeability in the Niger delta, while the Simandoux and Indonesian models are both suitable for shale corrections of fluid saturations.

Generally, results of this work indicate that the effective

porosity and saturation of formation water increases with increase in shale volume while, hydrocarbon saturation, and permeability decrease with increase in shale volume.

## CONFLICT OF INTERESTS

The authors have not declared any conflict of interests.

## REFERENCES

- Adeoti L, Ojo AA, Olatinsu OB, Fasakin OO, Adesanya OY (2015). Comparative Analysis Of Hydrocarbon Potential In Shaly Sand Reservoirs Using Archie And Simandoux Models: A Case Study Of "X" Field, Niger Delta, Nigeria. *Ife Journal of Science* 17:15-29.
- Agyingi CM, Agagu OK, Fozao KF, Njoh OA, Ngalla N (2013). Depositional patterns and hydrocarbon occurrence in middle to upper Miocene strata in part of the western Niger Delta Basin, Nigeria. *Journal of African Earth Sciences* 80:21-30.
- Aigbedion JA, Iyayi SE (2007). Formation evaluation of Oshioka field, using geophysical well logs, Middle-east Journal of Scientific Research 2:107-110.
- Alao PA, Ata AI, Nwoke CE (2013). Subsurface and Petrophysical Studies of Shaly-Sand Reservoir Targets in Apete Field, Niger Delta, ISRN Geophysics, Article ID 102450. <http://dx.doi.org/10.1155/2013/102450>.
- Asquith G, Gibson C (1982). *Basic Well Log Analysis and for Geologists*. AAPG, Tulsa, Oklahoma.
- Bijan M, Mehdi N, Hadi S, Yaser M (2010). Optimization of reservoir cut-off determination: a case study in SW Iran. *Petroleum Geoscience* 17:355-363.
- Buckles RS (1965). Correlating and averaging connate water saturation data. *Journal of Canadian Petroleum Technology* 9(1):42-52.
- Dejtrakulwong P, Mukerji T, Mavko G (2009). Investigating Thomas-Stieber model for property estimation of thin-bedded shaly-sand reservoirs, SEG Houston 2009 International Exposition and Annual Meeting, <http://library.seg.org/>
- Doust H (1990). Petroleum geology of the Niger Delta. Geological Society, London, Special Publications 50:365-365.
- Doust H, Omatsola E (1990). Niger delta, in *Divergent/Passive Margin Basins*, J. D. Edwards and P. A. Santogrossi, Eds., AAPG memoir, Tulsa. 48:239-248.
- Egeh EU, Okereke CS, Olagundoye OO (2001). Porosity and compaction trend in Okan field (Western Niger Delta) based on well log data. *Global Journal of Pure and Applied Sciences* 7:91-96.
- Ehrenberg SN, Eberli GP, Keramati M, Moallemi A (2006). Porosity-permeability relationships in interlayered limestone dolostone reservoirs. *American Association of Petroleum Geologists Bulletin* 90:91-114.
- Evamy DD, Haremboure J, Kamerling P, Knaap WA, Molloy FA, Rowlands PH (1978). Hydrocarbon habitat of Tertiary Niger Delta. *AAPG Bulletin* 62:1-39.
- Hamada GM (1999). An Integrated Approach to Determine Shale Volume and Hydrocarbon Potential in Shaly Sand, Proceedings of the SPWLA held in Houston, Texas, May-June, 1-25.
- Kulke H (1995). *Regional Petroleum Geology of the World. Part II: Africa, America, Australia and Antarctica*: Berlin, Gebruder Borntraeger. pp. 143-172.
- Kurniawan T (2002). Evaluation of the Hydrocarbon Potential in Low-Salinity Shaly Sand. Graduate Faculty of the Louisiana State University and Agricultural and Mechanical College, Louisiana, Unpublished Ph.D thesis.
- Larionov VV (1969). Borehole Radiometry, National Electric Drag Racing Association, Moscow, Soviet Union.
- Mæland AO (2014). Shaly Sand Petrophysics and its Impact on Full Field Reservoir Simulation Norwegian, Master Thesis Department of Petroleum Engineering and Applied Geophysics, University of Science and Technology.
- Moradi S, Moeini M, Ghassem Al-Askari MK, Mahvelati EH (2016). Determination of Shale Volume and Distribution Patterns and Effective Porosity from Well Log Data Based On Cross-Plot Approach for A Shaly Carbonate Gas Reservoir. *IOP Conf. Series: Earth and Environmental Science* 44:042002 <http://doi:10.1088/1755-1315/44/4/042002>.
- Nelson PH (1994). Permeability-Porosity Relationships in sedimentary rocks. *The Log Analyst* 35:38-62.
- Nwachukwu JI, Chukwurah PI (1986). Organic matter of Agbada Formation, Niger Delta, Nigeria. *American Association of Petroleum Geologists Bulletin* 70:48-55.
- Paul G (2018). Formation evaluation. Unpublished petrophysics Msc course Notes, University of Aberdeen, UK., <https://www.scribd.com/doc/110298097/Petrophysics-P-glover-1>, (Accessed 08-06-2018).
- Poupon A, Leveaux J (1971). Evaluation of Water Saturation in Shaly Formations, Trans. SPWLA 12th Annual Logging Symposium pp. 1-2.
- Selley RC, Morrill DC (1983). *The Reservoir*, International human resources development corporation, USA.
- Schlumberger (1972). *Log Interpretation, Volume I-Principles*. 1972 Edition, Schlumberger limited, 277 Park Avenue, New York, NY. 10017, pp. 43-58.
- Schlumberger (1989). *Log Interpretation, Principles and Applications*. Seventh printing. March 1998 © Schlumberger 1991, Schlumberger Wire line & Testing 225 Schlumberger Drive Sugar Land, Texas, 77478.
- Schlumberger (1997). *Log Interpretation Charts, Chart K 3*, 1997 Edition, Schlumberger wireline and Testing, P.O. Box 2175, Houston, Texas 77252-2175, pp. 4-39.
- Schlumberger (2009). *Log Interpretation Charts*, 2009 Edition. 225 Schlumberger Drive, Sugar Land, Texas 77478, pp. 268-270.
- Short KC, Stauble AJ (1967). *Outline of Geology of Niger Delta*. American Association of Petroleum Geologists Bulletin 51:761-799.
- Simandoux P (1963). Dielectric Measurements in Porous Media and Application to Shaly Formation, *Revue de l'Institut Français du Pétrole, Supplementary Issue*, pp. 193-215, (Translated text in SPWLA Reprint Volume Shaly Sand, July 1982).
- Stat Oil Research Group (2003). *Geological Reservoir Characterization. Research and Technology Memoir 4*.
- Thomas EC, Stieber SJ (1975). The distribution of shale in sandstones and its effect upon porosity: 16th Annual Logging Symposium, SPWLA, Paper T.
- Tixier MP (1949). Evaluation of permeability from electric log resistivity gradients. *The Oil and Gas Journal* 16:113-133.
- Toby D (2005). *Well Logging and Formation Evaluation*, Elsevier, Gulf Professional Publishing, USA.
- Ulasi I, Onyekuru O, Iwuagwu CJ (2012). Petrophysical Evaluation of Uzek Well using Well Log and Core Data, Offshore Depobelt, Niger Delta, Nigeria. *Advances in Applied Science Research* 3:1-26.

Appendix

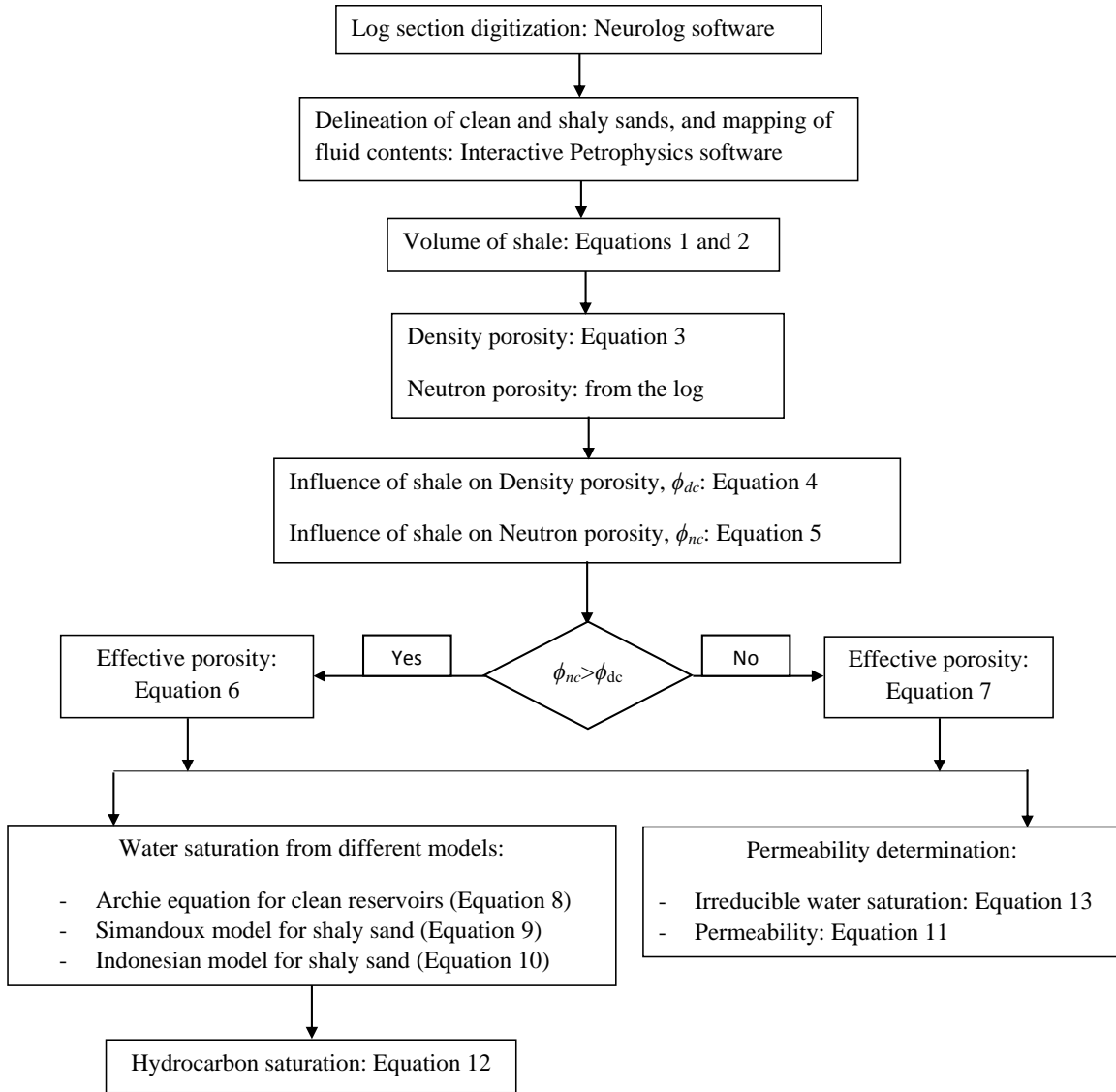


Figure A. The flow chart showing the sequence of procedures.